

# Connection-topology-dependent energy transport and ergotropy in quantum battery networks with reciprocal and nonreciprocal couplings

Bing-Bing Liu,<sup>1</sup> Rui Chen,<sup>2</sup> Jin-Lei Wu,<sup>1</sup> Gang Chen,<sup>1,\*</sup> and Shi-Lei Su<sup>1,†</sup>

<sup>1</sup>Quantum Information Institute, School of Physics and Laboratory of Zhongyuan Light, Zhengzhou University, Zhengzhou 450001, China

<sup>2</sup>School of Physics and Technology, Central China Normal University, Wuhan, Hubei 430072, China

(Dated: March 25, 2026)

The realization of scalable quantum battery architectures requires concern not only with how much energy can be stored, but also with how energy is transported, distributed, and converted into extractable work across connected battery nodes. While previous studies mainly focused on collective charging in multi-cell quantum batteries, the topology-dependent transport law and the corresponding work-oriented performance of quantum battery networks remain largely unexplored. In this work, we investigate quantum battery networks with engineered reciprocal and nonreciprocal couplings and compare different connection topologies, including cascaded and parallel architectures, within a unified transport framework. In the nonreciprocal regime, the optimal coupling follows distinct scaling laws for the two connection topologies, namely  $J_{\text{op}}^c \propto N$  for cascaded transport and  $J_{\text{op}}^p \propto N^{-1/2}$  for parallel charging in the large- $N$  limit. In reciprocal cascaded networks, a parity-dependent spectral response produces an odd-even transport effect that is absent in the nonreciprocal and parallel configurations. We further analyze the role of thermal and squeezed reservoirs and show that thermal noise mainly increases passive energy, whereas squeezing enhances ergotropy and thus the useful fraction of stored energy. These results shift the emphasis from charging enhancement to transport engineering and provide architecture-level design principles for quantum battery networks.

## I. INTRODUCTION

Quantum batteries, i.e., quantum systems engineered to store and release energy, have attracted broad interest because quantum coherence, correlations, and many-body effects can improve charging speed, charging power, and storage capability [1–10]. In addition to stored energy, the work-oriented figure of merit is the ergotropy, namely the maximum extractable work obtainable through unitary operations [11–13]. From this perspective, a useful quantum battery should be assessed not only by how much energy is accumulated, but also by how efficiently that energy can be delivered and converted into extractable work.

A broad range of charging protocols has been proposed, including feedback control charging [14–16], stimulated Raman adiabatic passage [17–19], and so on [20–28]. Multi-cell quantum batteries have been widely investigated for collective effects leading to superextensive charging advantages [29–33], including Dicke and Sachdev–Ye–Kitaev models, with two-photon Dicke batteries providing further power enhancement [34–41]. Moreover, quantum batteries are inevitably affected by decoherence and exhibit self-discharge effects [42]. Such detrimental influences can be mitigated by such as dark states [43] and Floquet engineering [44]. In particular, Ref. [45] shows that the unique hyperfine interaction of the  $^{14}\text{N}$  nucleus can enhance the ratio of coherent ergotropy, thereby improving the robustness against self-discharge.

In contrast to approaches focused on suppressing dissipation, noise-assisted and environment engineered mechanisms have emerged as effective routes for enhancing charging performance and mitigating degradation [46–57]. Nonrecipro-

city generated by cooperative dissipation has become a particularly promising ingredient because it enables broadband directional transport and suppresses backflow [58–62]. This mechanism has already been exploited to enhance the performance of quantum batteries [63–66]. Nonreciprocity has also been induced into the Dicke model and applied to enhance multi-cell batteries [67, 68].

However, previous studies primarily focused on quantum batteries composed of multiple cells; the role of network connectivity among batteries has not been fully explored. In realistic quantum technologies, energy storage is not to rely on a single battery unit; instead, multiple batteries are expected to be interconnected to form quantum battery networks [69, 70]. Such architectures are closer to practical quantum energy systems and naturally give rise to energy transport processes between different batteries, leading to richer dynamical behavior beyond that of isolated battery cells.

The present work addresses this next layer of the problem. Rather than focusing only on charging enhancement, we investigate how topology, transport directionality, and reservoir properties jointly determine energy delivery, steady-state storage, and ergotropy in quantum battery networks. We consider two representative architectures, cascaded and parallel, and derive analytical results that expose their distinct transport constraints. In particular, cascaded networks exhibit sequential delivery, while parallel networks exhibit collective redistribution. This distinction leads to opposite optimal-coupling trends with the battery number  $N$ :  $J_{\text{op}}^c \propto N$  and  $J_{\text{op}}^p \propto N^{-1/2}$  in the large- $N$  regime. We emphasize that our analysis establishes a general framework: the regimes discussed in Refs. [63, 65] correspond to parameter regions below and above the optimal coupling strength, respectively. It has also been extended to strong-coupling regime [71].

We further show that the reciprocal cascaded network exhibits a parity-dependent spectral transport mechanism, which

\* chengang971@163.com

† slsu@zzu.edu.cn

explains the odd-even dependence of the terminal-battery response and is absent in the nonreciprocal and parallel cases. Finally, reservoir properties are also important in determining the performance of quantum batteries [72–74]. By analyzing both thermal and squeezed reservoirs, we show that stored energy and ergotropy exhibit distinct environmental responses: thermal noise primarily increases the passive energy, whereas squeezing enhances the useful fraction of the stored energy. The present results provide insight into the mechanisms governing energy transport in quantum battery networks and may offer useful guidance for the design of scalable quantum energy storage architectures and future quantum energy networks.

## II. TRANSPORT MODEL AND OPTIMAL OPERATING POINT

We consider a system comprising  $N + 1$  cavity modes with the same resonance frequency  $\omega$ : one charger mode and  $N$  battery modes, as depicted in Fig. 1. The total Hamiltonian is written as  $H = H_I + H_c$ , where  $H_I$  describes the couplings among all nodes, and  $H_c = \epsilon(a + a^\dagger)$  is the classical drive applied to the charger. We investigate two representative network architectures, namely, cascaded and parallel connection topologies.

We first focus on the cascaded case, for which the corresponding Hamiltonian in the interaction picture takes the form

$$H_I = J_1 e^{i\theta_1} a^\dagger b_1 + \sum_{i < j=1}^N J_i e^{i\theta_i} b_i^\dagger b_j + \text{H.c.}, \quad (1)$$

with  $a$  and  $b_i$  denote the annihilation operators of the charger and  $i$ -th battery mode, and  $J_1$  ( $J_i$ ) and  $\theta_1$  ( $\theta_i$ ) represent the amplitude and phase of the coherent coupling.

Directional energy transport is induced by engineered non-reciprocal couplings mediated by cooperative dissipation [58, 63]. After adiabatic elimination of the reservoir degrees of freedom, the effective dynamics exhibits asymmetric energy transfer between different nodes of the quantum battery network. In the Markovian regime, the system dynamics is governed by the master equation

$$\frac{d\rho}{dt} = -i[H, \rho] + \kappa_a \mathcal{L}[a]\rho + \sum_{i=1}^N (\kappa_i \mathcal{L}[b_i]\rho + \mathcal{L}[q_i]\rho). \quad (2)$$

The dissipative superoperator  $\mathcal{L}[o]\rho = o\rho o^\dagger - 1/2\{o^\dagger o, \rho\}$ , where the collective jump operators associated with the shared reservoir are given by  $q_1 = \sqrt{\Gamma_1}(p_a a + p_{b_1} b_1)$ , and  $q_i = \sqrt{\Gamma_i}(p_{b_{i-1}} b_{i-1} + p_{b_i} b_i)$  for  $i \geq 2$ . Here,  $\kappa_a$  and  $\kappa_i$  are the local dissipation rates of the charger and battery modes into the independent baths, while  $\Gamma_i$  characterizes the strength of the cooperative dissipative coupling mediated by the shared reservoir.

Effective nonreciprocal coupling is engineered by balancing the dissipative interactions and the coherent coupling. Unidirectional energy transfer arises when the parameters satisfy  $\theta_i = \pi/2$ ,  $\mu_i = 1$ , or  $\theta_i = 0$ ,  $\mu_i = -i$ , and  $J_i = \Gamma_i/2$ ,

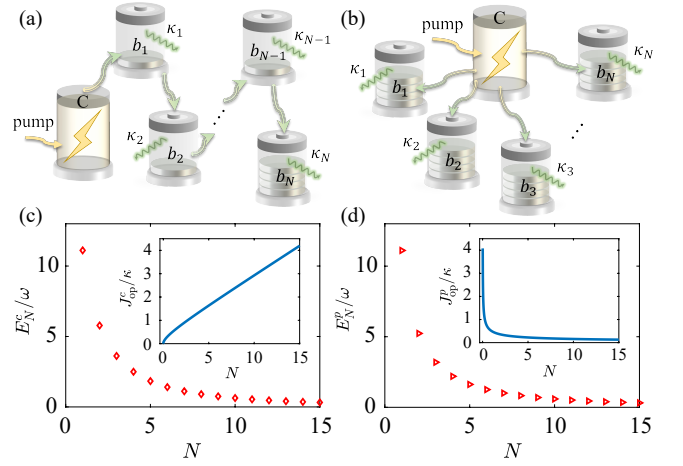


FIG. 1. Multi-body quantum batteries in the cascaded (a) and parallel (b) configurations, consisting of a charger (C) and  $N$  battery modes ( $b_i$ ). Steady-state stored energy as a function of the battery number  $N$  for cascaded (c) and parallel (d) schemes. Inset: optimal coupling strength  $J_{\text{op}}$  varies with  $N$ . The parameters used are  $\kappa/\omega = 0.003$ ,  $\epsilon/\omega = 0.01$ , and  $J = J_{\text{op}}$ .

where  $\mu_1 = p_a p_{b_1}$  and  $\mu_i = p_{b_{i-1}}^* p_{b_i}$ . The detailed derivation is presented in Appendix A.

The energy distribution can be obtained by solving the Heisenberg equations of motion, yielding an analytical expression for the energy distribution in the  $n$ -th battery

$$E_n(t) = \frac{\mathcal{A}_n}{\mathcal{V}_n^2} \left[ \mathcal{V}_n + \sum_{p=0}^n (-1)^{n+p} \left( \prod_{m \neq p}^n \Lambda_m \right) \mathcal{V}_n^{(p)} e^{-\Lambda_p t/2} \right]^2, \quad (3)$$

where

$$\mathcal{A}_n = \frac{4^{n+1} \omega \epsilon^2 \prod_{m=1}^n |\mu_m|^2 \Gamma_m^2}{\prod_{m=0}^n \Lambda_m^2},$$

and

$$\mathcal{V}_n \equiv \prod_{0 \leq m < j \leq n} (\Lambda_m - \Lambda_j),$$

$$\mathcal{V}_n^{(p)} \equiv \prod_{\substack{0 \leq m < j \leq n \\ m, j \neq p}} (\Lambda_m - \Lambda_j),$$

in which  $\Lambda_0 = \Gamma_1 |p_a|^2 + \kappa_a$ ,  $\Lambda_i = (\Gamma_i + \Gamma_{i+1}) |p_{b_i}|^2 + \kappa_{b_i}$ , for  $i = 1, \dots, n-1$ , and  $\Lambda_n = \Gamma_n |p_{b_n}|^2 + \kappa_{b_n}$ .

In the long-time limit  $t \rightarrow \infty$ , dissipation drives the system to relax to a steady state, for which the stored energy of the  $n$ -th battery reduces to

$$E_n^{\text{ss}} = \frac{4^{n+1} \omega \epsilon^2 \prod_{m=1}^n |\mu_m|^2 \Gamma_m^2}{\prod_{m=0}^n \Lambda_m^2}. \quad (4)$$

In the cascaded configuration, energy propagates sequentially from the charger toward the end of the chain. The terminal battery thus provides a natural figure of merit for transport performance, because it directly probes how much energy

survives the cumulative attenuation and leakage encountered along the chain. Exploiting the recursive structure revealed by the analytical results in Appendix A, the stored energy in the terminal battery can be expressed as

$$E_c^{\text{ss}}(N) = \frac{4^{N+1}\omega\varepsilon^2\Gamma^{2N}}{(\Gamma + \kappa)^4(2\Gamma + \kappa)^{2N-2}}, \quad (5)$$

where we have set  $\Gamma_i = \Gamma$ ,  $\kappa_i = \kappa$  for simplicity, which is consistent with the results reported in Ref. [65].

For the parallel charging configuration, the interaction Hamiltonian takes the form

$$H_I = \sum_{i=1}^N J_i e^{i\theta_i} a^\dagger b_i + \text{H.c.}, \quad (6)$$

where the cooperative dissipation via the shared reservoir is characterized by the collective jump operators  $q_i = \sqrt{\Gamma_i}(p_a a + p_{b_i} b_i)$ . The condition for nonreciprocity remains identical to that of the cascaded case, but with  $\mu_i = p_a p_{b_i}$ . Solving the corresponding dynamical equations yields the energy stored in the  $n$ -th battery,

$$E_n(t) = \frac{4^2\omega\varepsilon^2|\mu_n|^2\Gamma_n^2}{\Lambda_0^2\Lambda_n^2(\Lambda_0 - \Lambda_n)^2} \left[ (\Lambda_0 - \Lambda_n) - (\Lambda_0 e^{-\frac{\Lambda_0 t}{2}} - \Lambda_n e^{-\frac{\Lambda_n t}{2}}) \right]^2, \quad (7)$$

where  $\Lambda_0 = \sum_{i=1}^n \Gamma_i |p_a|^2 + \kappa_a$ ,  $\Lambda_i = \Gamma_i |p_{b_i}|^2 + \kappa_{b_i}$ , for  $i = 1, \dots, n$ . In the steady-state limit,

$$E_n^{\text{ss}} = \frac{4^2\omega\varepsilon^2|\mu_n|^2\Gamma_n^2}{\Lambda_1^2\Lambda_n^2}. \quad (8)$$

Similarly, combining the analytical results derived in Appendix A, the steady-state stored energy as a function of the battery number  $N$  can be obtained as

$$E_p^{\text{ss}}(N) = \frac{4^2\omega\varepsilon^2\Gamma^2}{(N\Gamma + \kappa)^2(\Gamma + \kappa)^2}. \quad (9)$$

The effective nonreciprocal coupling arises from the interplay between the coherent and dissipative interactions; there exists an optimal coupling strength  $J_{\text{op}}$  that maximizes the stored energy. By solving  $\partial E^{\text{ss}}/\partial J = 0$ , we can obtain

$$J_{\text{op}}^c(N) = \frac{\kappa}{8}(N + \sqrt{N^2 + 8N}), \quad J_{\text{op}}^p(N) = \frac{\kappa}{2\sqrt{N}}, \quad (10)$$

for the cascaded and parallel configurations, respectively. The corresponding maximal stored energies are shown in Fig. 1. Notably, the optimal coupling exhibits distinct scalings with the battery count  $N$  in the two configurations, increasing with propagation distance in the cascaded chain but decreasing with the number of simultaneously loaded nodes in the parallel geometry. This corresponds to the central result: the cascaded topology is characterized by sequential energy propagation, whereas the parallel topology is characterized by collective energy redistribution.

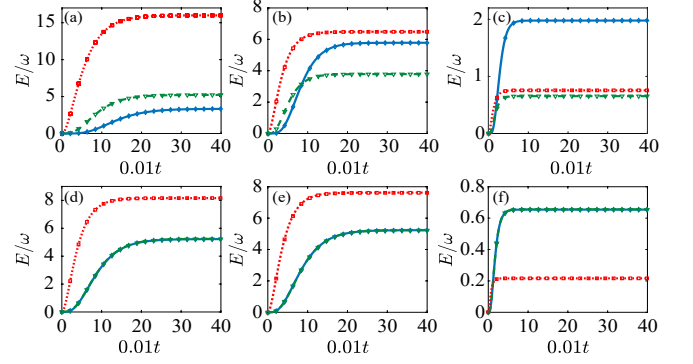


FIG. 2. Energy distribution across the charger and battery modes for different coupling strengths  $J/\omega = 0.001$  (a, d),  $J = J_{\text{op}}$  (b, e), and  $J/\omega = 0.01$  (c, f). The cascaded configuration is shown in (a)–(c), while the parallel configuration is shown in (d)–(f). Dotted, dashed, and solid curves represent the stored energy in the charger, the first battery, and the second battery, while markers denote the analytical results. The other parameters are  $\kappa/\omega = 0.003$ ,  $\varepsilon/\omega = 0.01$ , and  $N = 2$ .

In the large- $N$  limit, the optimal coupling exhibits qualitatively different scaling behaviors, with  $J_{\text{op}}^c \propto N$  and  $J_{\text{op}}^p \propto N^{-1/2}$ . In the cascaded architecture, the effective propagation distance increases with the number of batteries, resulting in progressively greater energy attenuation along the chain. Consequently, a larger coupling strength is required to maintain efficient energy delivery to the terminal node. In contrast, in the parallel configuration, the charging process exhibits a collective redistribution. Increasing the coupling strength enhances not only energy injection but also loss through the cooperative dissipation channel. Consequently, the optimal coupling  $J_{\text{op}}^p$  decreases with  $N$  due to the limitation of the nonreciprocity condition.

For  $J < J_{\text{op}}$ , the effective nonreciprocal coupling is too weak to extract energy from the charger. In this regime, the injected energy predominantly localizes in the charger, and only a small fraction is delivered to the battery. The coherent interaction is insufficient to overcome intrinsic local dissipation, thereby suppressing energy accumulation in the battery, as illustrated in Figs. 2(a) and (d). Moreover, our analytical results are in excellent agreement with the numerical calculations.

As  $J$  increases beyond  $J_{\text{op}}$ , the stronger coupling shortens the dynamical timescale, allowing the battery energy to approach its steady-state value more rapidly. However, this also amplifies cooperative (nonlocal) dissipative channels associated with the engineered nonreciprocal transmission. A substantial fraction of the injected energy is dissipated into the environment, resulting in reduced steady-state stored energy, as shown in Fig. 2. This behavior reflects a general trade-off between charging speed and energy storage efficiency under dissipative nonreciprocal interactions.

The optimal coupling  $J_{\text{op}}$  therefore corresponds to a balance between directional energy injection and environmental dissipation. At this point, nonreciprocity enables efficient energy transfer into the batteries while limiting both backflow and excessive leakage, thereby maximizing the steady-state

stored energy.

### III. RECIPROCAL AND NONRECIPROCAL TRANSPORT MECHANISMS

To obtain a more complete picture of energy transport in quantum battery networks, we now compare the reciprocal and nonreciprocal coupling cases. In contrast to directional transport, reciprocal interactions enable bidirectional energy flow and modal interference that significantly change how energy is distributed, which spectral features dominate the response, and how the steady state is approached.

For the reciprocal cascaded configuration, the internal transport exhibits a pronounced odd-even effect, leading to qualitatively different scaling laws for chains with odd and even numbers of batteries. For an odd number of batteries, the terminal stored energy is

$$E_N^{\text{ss}} = \omega \left[ \frac{2^{N+1} J^N \epsilon}{\sum_{j=0}^{(N+1)/2} a(j) J^{N+1-2j} \kappa^{2j}} \right]^2, \quad (11)$$

whereas for an even number of batteries it reads

$$E_N^{\text{ss}} = \omega \left[ \frac{2^{N+1} J^N \epsilon}{\sum_{j=0}^{N/2} b(j) J^{N-2j} \kappa^{2j+1}} \right]^2, \quad (12)$$

where  $a(j)$  and  $b(j)$  are the constants defined in Ref. [65]. By contrast, the reciprocal parallel configuration does not exhibit such parity-dependent transport, and its steady-state stored energy is

$$E_N^{\text{ss}} = \frac{4\Gamma^2 \omega \epsilon^2}{(4NJ^2 + \kappa^2)^2}. \quad (13)$$

At the optimal coupling  $J_{\text{op}}$ , the steady-state stored energy exhibits distinct behaviors for reciprocal and nonreciprocal interactions, as illustrated in Figs. 3(a) and 3(b). In the reciprocal cascaded coupling, the steady-state energy is strongly affected by the spectral structure of the underlying tight-binding Hamiltonian. In particular, the steady-state energy response can be expressed in terms of the Green function, whose modal contribution scales as  $(-E_k + i\kappa/2)^{-1}$ , see Appendix B for detailed discussion. As a result, eigenmodes with energies near zero acquire greater weight and therefore dominate the steady-state energy distribution. For the charging process of an even number of batteries, there always exists a zero-energy eigenmode; this mode makes a dominant contribution to the steady-state amplitude, enabling constructive energy transport from the charger to the end battery. In contrast, for an odd number of batteries, the spectrum is symmetric around zero energy, and no eigenmode exists. Contributions from different transport modes partially cancel due to interference, reducing the steady-state energy and giving rise to the observed odd-even imbalance in the energy distribution.

In addition, this spectral mechanism also determines the dependence of stored energy on the coupling strength. When  $N$  is odd, the stored energy exhibits a pronounced peak as a

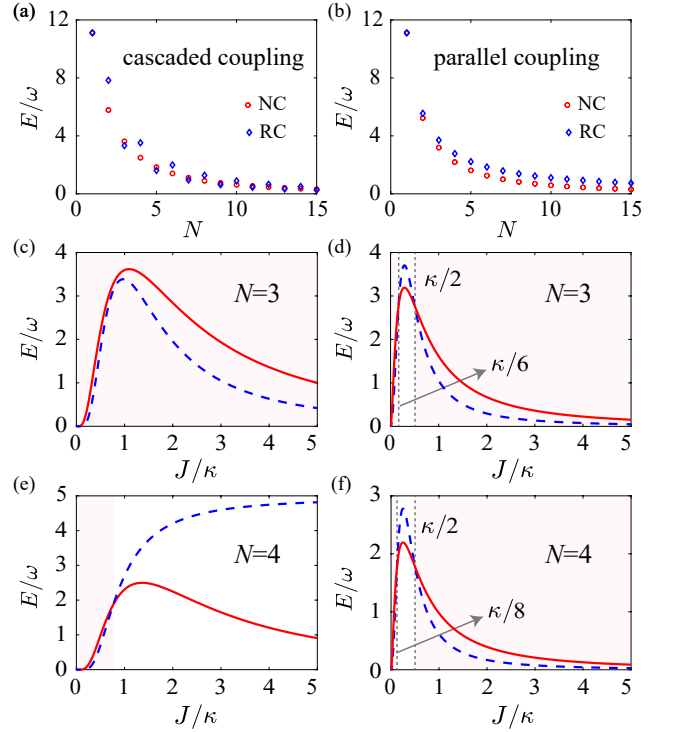


FIG. 3. Steady-state stored energy as a function of the battery number  $N$  under nonreciprocal coupling (NC) and reciprocal coupling (RC) for the cascaded (a) and parallel (b) configurations at  $J = J_{\text{op}}$ . Panels (c)–(f) show the steady-state stored energy versus the coupling strength  $J$ : the cascaded configuration in (c, e) and the parallel configuration in (d, f), with  $N = 3$  for (c, d) and  $N = 4$  for (e, f). The other parameters are  $\kappa/\omega = 0.003$ ,  $\epsilon/\omega = 0.01$ .

function of the coupling strength, as shown in Fig. 3(c). In the weak-coupling regime, energy transfer from the charger to the batteries is inefficient, resulting in low stored energy. As the coupling strength increases, the charger and the batteries hybridize into normal modes whose frequencies mismatch with the driving field. This detuning reduces charging efficiency and consequently decreases stored energy.

On the contrary, when  $N$  is even, the system supports a zero-energy mode that remains resonant with the driving field. As a result, there is no frequency mismatch induced by strong coupling. In this case, the stored energy increases with the coupling strength and ultimately approaches a saturation value, without decreasing, as shown in Fig. 3(e).

In contrast to the reciprocal systems, nonreciprocal coupling suppresses energy backflow; there always exists a peak as  $J$  changes. In the weak-coupling regime, the energy stored under nonreciprocal coupling is consistently higher than that under the reciprocal coupling case. Our results show that directional transport can enhance the steady-state stored energy over a broad parameter range.

For the parallel configuration, the transport spectrum does not support a zero-energy eigenmode, and the steady-state response therefore exhibits a much simpler structure than in the

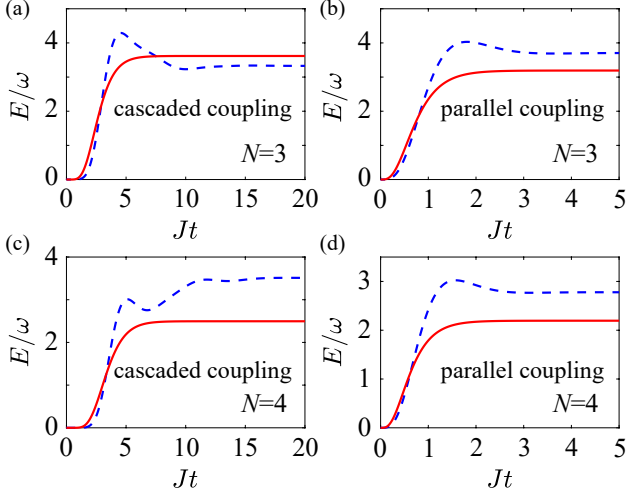


FIG. 4. Time evolution of the stored energy versus the scaled time for  $N = 3$  in (a, b), and  $N = 4$  in (c, d). The parameters are  $\kappa/\omega = 0.003$ ,  $\epsilon/\omega = 0.01$ , and  $J = J_{op}$ .

cascaded case. We identify a parameter window

$$\frac{\kappa}{2N} < J < \frac{\kappa}{2}, \quad (14)$$

within which reciprocal coupling can lead to a more efficient energy accumulation than in the nonreciprocal case. This regime, however, is relatively narrow, within which bidirectional energy exchange enhances the effective hybridization between the charger and the batteries, as shown in Figs. 3(d) and (f). Outside this window, the directional-transport advantage of the nonreciprocal architecture is restored.

We further compare the charging dynamics for different coupling configurations, as shown in Fig. 4. The steady-state energy quantifies how much energy is eventually stored, but it does not specify how rapidly the network reaches its operating point. In the reciprocal cascaded configuration, energy propagates sequentially along the chain. Oscillatory exchange between neighboring cavities slows down the net energy transfer, resulting in a longer relaxation time that increases approximately linearly with the number of batteries  $N$ . In contrast, in the parallel configuration, the charger injects energy into all batteries simultaneously, making the relaxation time much shorter and nearly independent of  $N$ .

The situation changes qualitatively for nonreciprocal coupling. In this case, energy is delivered monotonically from the charger to the batteries, the dwell time in intermediate nodes is reduced, and the relaxation toward the steady state is accelerated. In this sense, the nonreciprocal network improves not only the steady-state terminal energy, but also the transport power.

#### IV. RESERVOIR CONSIDERATION

Because the nonreciprocal coupling is mediated by a shared reservoir, it is important to examine how its properties affect

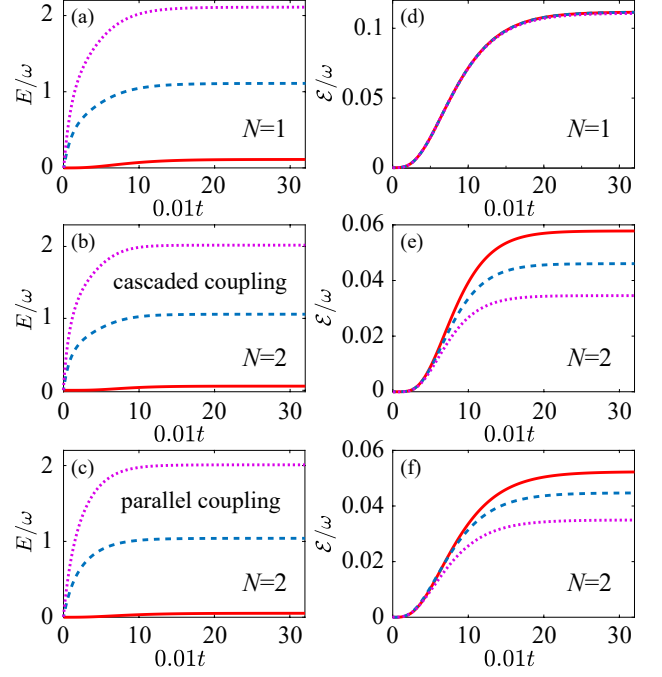


FIG. 5. Charging dynamics of Stored energy and ergotrop. Top row: single battery ( $N = 1$ ). Middle row: cascaded configuration with  $N = 2$ . Bottom row: parallel configuration with  $N = 2$ . The solid line, the dashed line, and the dotted line represent  $n_{th} = 0$ ,  $n_{th} = 1$ , and  $n_{th} = 2$ , respectively. The other parameters are  $\kappa/\omega = 0.003$ ,  $\epsilon/\omega = 0.001$ , and  $J = J_{op}$ .

the charging performance. We first consider a thermal environment, for which the system dynamics is described by the following master equation

$$\begin{aligned} \dot{\rho} = & -i[H, \rho] + n_{th} \left[ \kappa_a \mathcal{L}[a^\dagger] \rho + \sum_{i=1}^N (\kappa_i \mathcal{L}[b_i^\dagger] \rho + \mathcal{L}[q_i^\dagger] \rho) \right] \\ & + (n_{th} + 1) \left[ \kappa_a \mathcal{L}[a] \rho + \sum_{i=1}^N (\kappa_i \mathcal{L}[b_i] \rho + \mathcal{L}[L_{q_i}] \rho) \right], \end{aligned} \quad (15)$$

where  $n_{th}$  is the average number of photons in the reservoir. As illustrated in Fig. 5, we plot the time evolution of the stored energy in the quantum battery. In the thermal bath, environment-induced excitations continuously inject into the cavity mode via Lindblad processes. The fluctuation strength associated with the thermal reservoir scales linearly with the bath occupation, the induced incoherent pumping of photons into the system is correspondingly enhanced, resulting in a steady-state energy that increases linearly with  $n_{th}$ , which can be expressed as

$$E_{c(p)}^{ss'} = E_{c(p)}^{ss} + n_{th},$$

for both cascaded and parallel topologies. We note that, due to the rapid growth of the Hilbert-space dimension with increasing driving strength, our simulations are performed at a relatively weak drive to ensure convergence in a truncated Fock

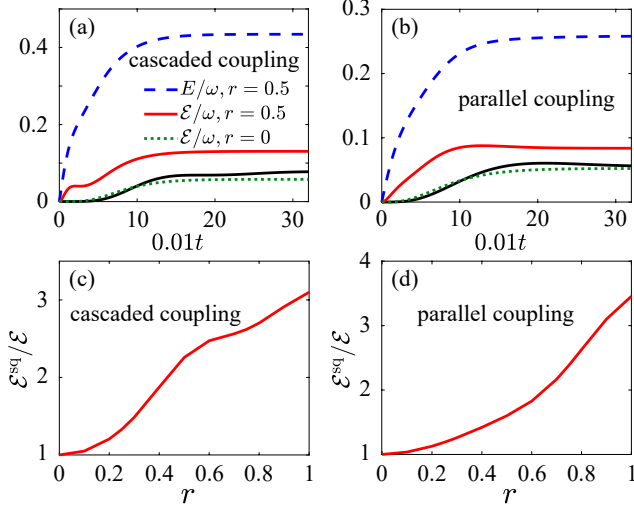


FIG. 6. Time evolution of the stored energy and ergotropy under nonreciprocal coupling for the cascaded (a) and parallel (b) configurations. Black solid curves correspond to reciprocal coupling for comparison. Enhancement factor of the ergotropy,  $\mathcal{E}^{\text{sq}}/\mathcal{E}$ , as a function of the squeezing parameter  $r$  for the cascaded (c) and parallel (d) configurations. Here,  $\mathcal{E}^{\text{sq}}$  denotes the ergotropy in the presence of squeezing, while  $\mathcal{E}$  corresponds to the case without squeezing. The parameters are  $\kappa/\omega = 0.003$ ,  $\epsilon/\omega = 0.001$ ,  $J = J_{\text{op}}$ , and  $N = 2$ .

space. The resulting finite-dimensional truncation may induce minor quantitative deviations without modifying the qualitative behavior of the results.

However, not all of the stored energy can be utilized; ergotropy (extractable work), defined as  $\mathcal{E} = \langle b^\dagger b \rangle - \min_U \langle U b^\dagger b U^\dagger \rangle$ , is used to quantify the performance of the battery [3, 75, 76]. For a zero-temperature reservoir, the initial state of the battery corresponds to the ground state, and the system remains in a pure state throughout the evolution process. As a result,  $\mathcal{E}$  is equivalent to the energy of the system [77, 78]. In contrast, a hot reservoir drives the system toward mixed states due to thermal fluctuations. Although thermal excitations can increase the total population  $\langle b^\dagger b \rangle$ , they mainly contribute disordered energy that cannot be efficiently converted into useful work. As a result, the enhancement of stored energy does not necessarily translate into improved battery performance, and the ergotropy may even be reduced in the presence of thermal noise.

As shown in Figs. 5(d-f), the ergotropy in the hot reservoir is lower than that in the vacuum-reservoir case, and decreases as the reservoir temperature increases. This behavior originates from the fact that thermal fluctuations primarily inject incoherent excitations into the system. These results indicate that, while thermal environments can enhance overall energy storage, low-temperature reservoirs are more favorable for preserving coherent energy accumulation and maintaining a larger extractable fraction, highlighting the distinction between energy storage and useful work extraction in quantum batteries.

We further consider the effect of a squeezed reservoir. The

dynamics of the system is described by

$$\begin{aligned} \dot{\rho} = & -i[H, \rho] + P \left[ \kappa_a \mathcal{L}[a^\dagger] \rho + \sum_{i=1}^N (\kappa_i \mathcal{L}[b_i^\dagger] \rho + \mathcal{L}[q_i^\dagger] \rho) \right] \\ & + (P+1) \left[ \kappa_a \mathcal{L}[a] \rho + \sum_{i=1}^N (\kappa_i \mathcal{L}[b_i] \rho + \mathcal{L}[L_{q_i}] \rho) \right] \\ & - Q \left[ \kappa_a \mathcal{L}'[a] \rho + \sum_{i=1}^N (\kappa_i \mathcal{L}'[b_i] \rho + \mathcal{L}'[L_{q_i}] \rho) \right] \\ & - Q^* \left[ \kappa_a \mathcal{L}'[a^\dagger] \rho + \sum_{i=1}^N (\kappa_i \mathcal{L}'[b_i^\dagger] \rho + \mathcal{L}'[q_i^\dagger] \rho) \right], \quad (16) \end{aligned}$$

where  $\mathcal{L}'[o] \rho = o \rho o - 1/2 \{o o, \rho\}$ ,  $P = \sinh^2 r$ , and  $Q = \sinh r \cosh r e^{-i\theta_r}$ , with  $r$  and  $\theta_r$  represent the squeezing strength and phase. Unlike the thermal bath, the squeezed reservoir not only provides excitations but also introduces quantum correlations through two-photon processes. These correlations modify the fluctuation properties of the environment and convert environmental fluctuations into ordered energy that can be extracted through unitary operations. As illustrated in Fig. 6, the squeezed reservoir enhances the ergotropy of the quantum battery. Moreover, the extractable work increases with the squeezing strength, demonstrating that stronger squeezing not only increases the stored energy but also enhances the useful fraction.

## V. DESIGN PRINCIPLES AND FEASIBLE IMPLEMENTATION

Our work extends single-cell quantum batteries by incorporating spatial transport effects and establishes transport-oriented design rules for battery networks. First, topology determines the main transport constraint: cascaded chains exhibit sequential energy propagation, whereas parallel networks exhibit collective energy redistribution. Second, coupling directionality controls energy backflow and modal interference, making nonreciprocal interactions particularly advantageous for fast relaxation. Third, reservoir properties determine whether the transported energy remains passive or becomes extractable work: thermal noise mainly raises passive energy, whereas squeezing enhances nonpassive storage and ergotropy.

Arrays of coupled optical or microwave cavities provide a natural platform for implementing the proposed architectures, since both coherent hopping and engineered dissipation can be precisely controlled. Effective nonreciprocal coupling can be achieved by engineering collective dissipation via strongly damped auxiliary-cavity modes. After adiabatic elimination of these auxiliary degrees of freedom, an effective cooperative dissipative coupling emerges, giving rise to directional energy transport. This offers a feasible route toward realizing nonreciprocal quantum battery networks using existing photonic and superconducting cavity technologies.

## VI. CONCLUSION

In conclusion, we have studied how topology, transport directionality, and reservoir type jointly determine energy delivery and work-oriented performance in quantum battery networks. For cascaded and parallel architectures, we derived analytical results that revealed distinct topology-dependent optimal-coupling laws, reflecting the contrast between sequential-delivery transport and collective-redistribution charging. We further showed that reciprocal cascaded networks exhibit a parity-dependent spectral transport mechanism, which explains the odd-even terminal-energy response and is absent in the nonreciprocal and parallel configurations. Finally, by comparing thermal and squeezed reservoirs, we demonstrated that stored energy and ergotropy can respond qualitatively differently to the environment: thermal noise mainly increases passive energy, whereas squeezing enhances extractable work. These results emphasize transport engineering and work extraction, and they provide a clearer framework for designing quantum battery networks.

## ACKNOWLEDGMENTS

This work was supported by the National Key R&D Program of China (Grants No. 2022YFA1404500), the National Natural Science Foundation of China (Grants No. 12274376, No. 12575032, No. 12125406, No. U24A2015), and the Natural Science Foundation of Henan Province under Grant No. 232300421075.

## DATA AVAILABILITY

The data that support the findings of this article are openly available [79].

## Appendix A: Analytical solution of the charging dynamics for cascaded and parallel configurations

We first consider a minimal system to illustrate the analytical procedure; this structure enables the analytical results to be extended straightforwardly to an arbitrary number of batteries.

### 1. Cascaded configuration

For the cascaded coupling with  $N = 2$ , the equations of motion for the first moments read

$$\begin{aligned}\frac{d\langle a \rangle}{dt} &= -\frac{\Lambda_0}{2}\langle a \rangle - (iJ_1 e^{i\theta_1} + \frac{\mu_1 \Gamma_1}{2}\langle b_1 \rangle) - i\epsilon, \\ \frac{d\langle b_1 \rangle}{dt} &= -\frac{\Lambda_1}{2}\langle b_1 \rangle - (iJ_1 e^{-i\theta_1} + \frac{\mu_1^* \Gamma_1}{2}\langle a \rangle) - (iJ_2 e^{i\theta_2} \\ &\quad + \frac{\mu_2 \Gamma_2}{2}\langle b_2 \rangle), \\ \frac{d\langle b_2 \rangle}{dt} &= -\frac{\Lambda_2}{2}\langle b_2 \rangle - (iJ_2 e^{-i\theta_2} + \frac{\mu_2^* \Gamma_2}{2}\langle b_1 \rangle),\end{aligned}\quad (\text{A1})$$

where  $\mu_1 = p_a^* p_b$ ,  $\mu_2 = p_{b_1}^* p_{b_2}$ , and  $\Lambda_0 = \Gamma_1 |p_a|^2 + \kappa_a$ ,  $\Lambda_1 = (\Gamma_1 + \Gamma_2) |p_{b_1}|^2 + \kappa_{b_1}$ ,  $\Lambda_2 = \Gamma_2 |p_{b_2}|^2 + \kappa_{b_2}$ . Nonreciprocal coupling can be realized when  $\theta_1 = \theta_2 = \pi/2$ ,  $p_a = 1$ ,  $p_{b_1} = 1$ ,  $p_{b_2} = 1$ , or  $\theta_1 = \theta_2 = 0$ ,  $p_a = i$ ,  $p_{b_1} = 1$ ,  $p_{b_2} = -i$ , and  $J_i = \Gamma_i/2$ .

Solving the above linear system yields the stored energies

$$\begin{aligned}E_a(t) &= |\langle a \rangle|^2 = \frac{4\omega\epsilon^2(1 - e^{-\frac{1}{2}t\Lambda_0})^2}{\Lambda_0^2}, \\ E_{b_1}(t) &= |\langle b_1 \rangle|^2 = \frac{16\omega\epsilon^2|\mu_1|^2\Gamma_1^2}{\Lambda_0^2\Lambda_1^2(\Lambda_0 - \Lambda_1)^2} \left[ (\Lambda_0 - \Lambda_1) \right. \\ &\quad \left. - (\Lambda_0 e^{-\frac{1}{2}\Lambda_1 t} - \Lambda_1 e^{-\frac{1}{2}\Lambda_0 t}) \right]^2, \\ E_{b_2}(t) &= |\langle b_2 \rangle|^2 \\ &= \frac{64\omega\epsilon^2|\mu_1|^2|\mu_2|^2\Gamma_1^2\Gamma_2^2}{\Lambda_0^2\Lambda_1^2\Lambda_2^2(\Lambda_0 - \Lambda_1)^2(\Lambda_1 - \Lambda_2)^2(\Lambda_0 - \Lambda_2)^2} \\ &\quad \times \left[ (\Lambda_0 - \Lambda_1)(\Lambda_1 - \Lambda_2)(\Lambda_0 - \Lambda_2) - \Lambda_0\Lambda_1 \right. \\ &\quad \times (\Lambda_0 - \Lambda_1)e^{-\frac{1}{2}\Lambda_2 t} + \Lambda_0\Lambda_2(\Lambda_0 - \Lambda_2)e^{-\frac{1}{2}\Lambda_1 t} \\ &\quad \left. - \Lambda_1\Lambda_2(\Lambda_1 - \Lambda_2)e^{-\frac{1}{2}\Lambda_0 t} \right]^2.\end{aligned}\quad (\text{A2})$$

For  $N = 3$ , the equations of motion are given by

$$\begin{aligned}\frac{d\langle a \rangle}{dt} &= -\frac{\Lambda_0}{2}\langle a \rangle - (iJ_1 e^{i\theta_1} + \frac{\mu_1 \Gamma_1}{2}\langle b_1 \rangle) - i\epsilon \\ \frac{d\langle b_1 \rangle}{dt} &= -\frac{\Lambda_1}{2}\langle b_1 \rangle - (iJ_1 e^{-i\theta_1} + \frac{\mu_1^* \Gamma_1}{2}\langle a \rangle) - (iJ_2 e^{i\theta_2} \\ &\quad + \frac{\mu_2 \Gamma_2}{2}\langle b_2 \rangle) \\ \frac{d\langle b_2 \rangle}{dt} &= -\frac{\Lambda_2}{2}\langle b_2 \rangle - (iJ_2 e^{-i\theta_2} + \frac{\mu_2^* \Gamma_2}{2}\langle b_1 \rangle) - (iJ_3 e^{i\theta_3} \\ &\quad + \frac{\mu_3 \Gamma_3}{2}\langle b_3 \rangle) \\ \frac{d\langle b_3 \rangle}{dt} &= -\frac{\Lambda_3}{2}\langle b_3 \rangle - (iJ_3 e^{-i\theta_3} + \frac{\mu_3^* \Gamma_3}{2}\langle b_2 \rangle),\end{aligned}\quad (\text{A3})$$

where  $\mu_1 = p_a^* p_b$ ,  $\mu_2 = p_{b_1}^* p_{b_2}$ ,  $\mu_3 = p_{b_2}^* p_{b_3}$ , and  $\Lambda_0 = \Gamma_1 |p_a|^2 + \kappa_a$ ,  $\Lambda_1 = (\Gamma_1 + \Gamma_2) |p_{b_1}|^2 + \kappa_{b_1}$ ,  $\Lambda_2 = (\Gamma_2 + \Gamma_3) |p_{b_2}|^2 + \kappa_{b_2}$ ,  $\Lambda_3 = \Gamma_3 |p_{b_3}|^2 + \kappa_{b_3}$ . Nonreciprocal coupling can be realized by setting  $\theta_1 = \theta_2 = \theta_3 = \pi/2$ ,  $p_a = p_{b_1} = p_{b_2} = p_{b_3} = 1$ , or  $\theta_1 = \theta_2 = \theta_3 = 0$ ,  $p_a = i$ ,  $p_{b_1} = 1$ ,  $p_{b_2} = -i$ ,  $p_{b_3} = -1$ , and  $J_i = \Gamma_i/2$ .

The corresponding stored energies read

$$\begin{aligned}
E_a(t) &= |\langle a \rangle|^2 = \frac{4\omega\varepsilon^2(1 - e^{-\frac{1}{2}t\Lambda_0})^2}{\Lambda_0^2}, \\
E_{b_1}(t) &= |\langle b_1 \rangle|^2 = \frac{16\omega\varepsilon^2|\mu_1|^2\Gamma_1^2}{\Lambda_0^2\Lambda_1^2(\Lambda_0 - \Lambda_1)^2} \left[ (\Lambda_0 - \Lambda_1) \right. \\
&\quad \left. - (\Lambda_0 e^{-\frac{1}{2}\Lambda_1 t} - \Lambda_1 e^{-\frac{1}{2}\Lambda_0 t}) \right]^2, \\
E_{b_2}(t) &= |\langle b_2 \rangle|^2 \\
&= \frac{64\omega\varepsilon^2|\mu_1|^2|\mu_2|^2\Gamma_1^2\Gamma_2^2}{\Lambda_0^2\Lambda_1^2\Lambda_2^2(\Lambda_0 - \Lambda_1)^2(\Lambda_1 - \Lambda_2)^2(\Lambda_0 - \Lambda_2)^2} \\
&\quad \left[ (\Lambda_0 - \Lambda_1)(\Lambda_1 - \Lambda_2)(\Lambda_0 - \Lambda_2) - \Lambda_0\Lambda_1 \right. \\
&\quad \times (\Lambda_0 - \Lambda_1)e^{-\frac{1}{2}\Lambda_2 t} + \Lambda_0\Lambda_2(\Lambda_0 - \Lambda_2)e^{-\frac{1}{2}\Lambda_1 t} \\
&\quad \left. - \Lambda_1\Lambda_2(\Lambda_1 - \Lambda_2)e^{-\frac{1}{2}\Lambda_0 t} \right]^2. \\
E_{b_3}(t) &= |\langle b_3 \rangle|^2 \\
&= \frac{256\omega\varepsilon^2|\mu_1|^2|\mu_2|^2|\mu_3|^2\Gamma_1^2\Gamma_2^2\Gamma_3^2}{\Lambda_0^2\Lambda_1^2\Lambda_2^2\Lambda_3^2(\Lambda_0 - \Lambda_1)^2(\Lambda_0 - \Lambda_2)^2(\Lambda_0 - \Lambda_3)^2} \\
&\quad \times \frac{1}{(\Lambda_1 - \Lambda_2)^2(\Lambda_1 - \Lambda_3)^2(\Lambda_2 - \Lambda_3)^2} \\
&\quad \times \left[ (\Lambda_0 - \Lambda_1)(\Lambda_0 - \Lambda_2)(\Lambda_0 - \Lambda_3)(\Lambda_1 - \Lambda_2) \right. \\
&\quad \times (\Lambda_1 - \Lambda_3)(\Lambda_2 - \Lambda_3) \\
&\quad - \Lambda_0\Lambda_1\Lambda_2(\Lambda_0 - \Lambda_1)(\Lambda_0 - \Lambda_2)(\Lambda_1 - \Lambda_2)e^{-\frac{\Lambda_3 t}{2}} \\
&\quad + \Lambda_0\Lambda_1\Lambda_3(\Lambda_0 - \Lambda_1)(\Lambda_0 - \Lambda_3)(\Lambda_1 - \Lambda_3)e^{-\frac{\Lambda_2 t}{2}} \\
&\quad - \Lambda_0\Lambda_2\Lambda_3(\Lambda_0 - \Lambda_2)(\Lambda_0 - \Lambda_3)(\Lambda_2 - \Lambda_3)e^{-\frac{\Lambda_1 t}{2}} \\
&\quad \left. + \Lambda_1\Lambda_2\Lambda_3(\Lambda_1 - \Lambda_2)(\Lambda_1 - \Lambda_3)(\Lambda_2 - \Lambda_3)e^{-\frac{\Lambda_0 t}{2}} \right]^2. \tag{A4}
\end{aligned}$$

## 2. Parallel configuration

In the parallel configuration, the charger couples to all battery modes simultaneously. For  $N = 2$ , the operator equations become

$$\begin{aligned}
\frac{d\langle a \rangle}{dt} &= -\frac{\Lambda_0}{2}\langle a \rangle - (iJ_1 e^{i\theta_1} + \frac{\mu_1\Gamma_1}{2})\langle b_1 \rangle \\
&\quad - (iJ_1 e^{i\theta_1} + \frac{\mu_2\Gamma_2}{2})\langle b_2 \rangle - i\varepsilon \\
\frac{d\langle b_1 \rangle}{dt} &= -\frac{\Lambda_1}{2}\langle b_1 \rangle - (iJ_1 e^{-i\theta_1} + \frac{\mu_1^*\Gamma_1}{2})\langle a \rangle \\
\frac{d\langle b_2 \rangle}{dt} &= -\frac{\Lambda_2}{2}\langle b_2 \rangle - (iJ_2 e^{-i\theta_2} + \frac{\mu_2^*\Gamma_2}{2})\langle a \rangle \tag{A5}
\end{aligned}$$

where  $\mu_1 = p_a^* p_{b_1}$ ,  $\mu_2 = p_a^* p_{b_2}$  and  $\Lambda_0 = \kappa_a + (\Gamma_1 + \Gamma_2)|p_a|^2$ ,  $\Lambda_1 = \kappa_{b_1} + \Gamma_1|p_{b_1}|^2$  and  $\Lambda_2 = \kappa_{b_2} + \Gamma_2|p_{b_2}|^2$ . Nonreciprocal coupling can be realized when  $\theta_1 = \theta_2 = \pi/2$ ,  $p_a = p_{b_1} =$

$p_{b_2} = 1$ , or  $\theta_1 = \theta_2 = 0$ ,  $p_a = i$ ,  $p_{b_1} = p_{b_2} = 1$ , and  $J_i = \Gamma_i/2$ .

The corresponding stored energies are

$$\begin{aligned}
E_a(t) &= \frac{4\omega\varepsilon^2(1 - e^{-\frac{1}{2}t\Lambda_0})^2}{\Lambda_0^2}, \\
E_{b_1}(t) &= \frac{16\omega\varepsilon^2|\mu_1|^2\Gamma_1^2}{\Lambda_0^2\Lambda_1^2(\Lambda_0 - \Lambda_1)^2} \left[ (\Lambda_0 - \Lambda_1) - (\Lambda_0 e^{-\frac{1}{2}\Lambda_1 t} \right. \\
&\quad \left. - \Lambda_1 e^{-\frac{1}{2}\Lambda_0 t}) \right]^2, \\
E_{b_2}(t) &= \frac{16\omega\varepsilon^2|\mu_2|^2\Gamma_2^2}{\Lambda_0^2\Lambda_2^2(\Lambda_0 - \Lambda_2)^2} \left[ (\Lambda_0 - \Lambda_2) - (\Lambda_0 e^{-\frac{1}{2}\Lambda_2 t} \right. \\
&\quad \left. - \Lambda_2 e^{-\frac{1}{2}\Lambda_0 t}) \right]^2. \tag{A6}
\end{aligned}$$

For  $N = 3$ , there have

$$\begin{aligned}
\frac{d\langle a \rangle}{dt} &= -\frac{\Lambda_0}{2}\langle a \rangle - (iJ_1 e^{i\theta_1} + \frac{\mu_1\Gamma_1}{2})\langle b_1 \rangle \\
&\quad - (iJ_2 e^{i\theta_2} + \frac{\mu_2\Gamma_2}{2})\langle b_2 \rangle - (iJ_3 e^{i\theta_3} \\
&\quad + \frac{\mu_3\Gamma_3}{2})\langle b_3 \rangle - i\varepsilon \\
\frac{d\langle b_1 \rangle}{dt} &= -\frac{\Lambda_1}{2}\langle b_1 \rangle - (iJ_1 e^{-i\theta_1} + \frac{\mu_1^*\Gamma_1}{2})\langle a \rangle \\
\frac{d\langle b_2 \rangle}{dt} &= -\frac{\Lambda_2}{2}\langle b_2 \rangle - (iJ_2 e^{-i\theta_2} + \frac{\mu_2^*\Gamma_2}{2})\langle a \rangle \\
\frac{d\langle b_3 \rangle}{dt} &= -\frac{\Lambda_3}{2}\langle b_3 \rangle - (iJ_3 e^{-i\theta_3} + \frac{\mu_3^*\Gamma_3}{2})\langle a \rangle, \tag{A7}
\end{aligned}$$

where  $\mu_1 = p_a^* p_{b_1}$ ,  $\mu_2 = p_a^* p_{b_2}$ ,  $\mu_3 = p_a^* p_{b_3}$  and  $\Lambda_0 = \kappa_a + (\Gamma_1 + \Gamma_2 + \Gamma_3)|p_a|^2$ ,  $\Lambda_1 = \kappa_{b_1} + \Gamma_1|p_{b_1}|^2$ ,  $\Lambda_2 = \kappa_{b_2} + \Gamma_2|p_{b_2}|^2$ , and  $\Lambda_3 = \kappa_{b_3} + \Gamma_3|p_{b_3}|^2$ . Nonreciprocal coupling can be realized by setting  $\theta_1 = \theta_2 = \theta_3 = \pi/2$ ,  $p_a = p_{b_1} = p_{b_2} = p_{b_3} = 1$ , or  $\theta_1 = \theta_2 = \theta_3 = 0$ ,  $p_a = i$ ,  $p_{b_1} = p_{b_2} = p_{b_3} = 1$ , and  $J_i = \Gamma_i/2$ .

The corresponding stored energies are

$$\begin{aligned}
E_a(t) &= \frac{4\omega\varepsilon^2(1 - e^{-\frac{1}{2}t\Lambda_0})^2}{\Lambda_0^2}, \\
E_{b_1}(t) &= \frac{16\omega\varepsilon^2|\mu_1|^2\Gamma_1^2}{\Lambda_0^2\Lambda_1^2(\Lambda_0 - \Lambda_1)^2} \left[ (\Lambda_0 - \Lambda_1) - (\Lambda_0 e^{-\frac{1}{2}\Lambda_1 t} \right. \\
&\quad \left. - \Lambda_1 e^{-\frac{1}{2}\Lambda_0 t}) \right]^2, \\
E_{b_2}(t) &= \frac{16\omega\varepsilon^2|\mu_2|^2\Gamma_2^2}{\Lambda_0^2\Lambda_2^2(\Lambda_0 - \Lambda_2)^2} \left[ (\Lambda_0 - \Lambda_2) - (\Lambda_0 e^{-\frac{1}{2}\Lambda_2 t} \right. \\
&\quad \left. - \Lambda_2 e^{-\frac{1}{2}\Lambda_0 t}) \right]^2, \\
E_{b_3}(t) &= \frac{16\omega\varepsilon^2|\mu_3|^2\Gamma_3^2}{\Lambda_0^2\Lambda_3^2(\Lambda_0 - \Lambda_3)^2} \left[ (\Lambda_0 - \Lambda_3) - (\Lambda_0 e^{-\frac{1}{2}\Lambda_3 t} \right. \\
&\quad \left. - \Lambda_3 e^{-\frac{1}{2}\Lambda_0 t}) \right]^2. \tag{A8}
\end{aligned}$$

The optimal effective coupling can be obtained by maximizing the steady-state stored energy with respect to the dissipative coupling strength, i.e.,

$$\frac{\partial E_c^{\text{ss}}(N)}{\partial J} = -\frac{2^{3+2N}\omega\Gamma^{-1+2N}\epsilon^2}{(\Gamma+\kappa)^5}(2\Gamma+\kappa)^{1-2N}(2\Gamma^2 - N\Gamma\kappa - N\kappa^2) = 0, \quad (\text{A9})$$

and

$$\frac{\partial E_p^{\text{ss}}}{\partial J} = \frac{32\omega\Gamma\epsilon^2(-N\Gamma^2 + \kappa^2)}{(\Gamma+\kappa)^3(N\Gamma+\kappa)^3} = 0. \quad (\text{A10})$$

which leads to the analytical expressions in the main text.

These results explicitly reveal how directional transport and cooperative dissipation determine the scaling of the stored energy with the battery number.

### Appendix B: Analytical proof of the energy difference between odd and even battery chains under reciprocal coupling

In this appendix, we analyze the origin of the energy difference between odd and even battery chains under reciprocal coupling. We consider a charger coupled to a chain of  $N$  quantum batteries with nearest-neighbor reciprocal coupling, described by the Hamiltonian

$$H = \epsilon(a + a^\dagger) + Ja^\dagger b_1 + \sum_{i<j=1}^N Jb_i^\dagger b_j + \text{H.c.}, \quad (\text{B1})$$

Including uniform dissipation  $\kappa$ , the steady-state amplitudes satisfy the set of linear equations

$$\begin{aligned} \frac{i\kappa}{2}a - Jb_1 &= \epsilon, \\ \frac{i\kappa}{2}b_1 - J(a + b_2) &= 0, \\ \frac{i\kappa}{2}b_2 - J(b_1 + b_3) &= 0, \\ &\vdots \\ \frac{i\kappa}{2}b_N - Jb_{N-1} &= 0. \end{aligned} \quad (\text{B2})$$

Defining the vector  $\mathbf{a} = (a, b_1, b_2, \dots, b_N)^T$ , the steady state equation can be written as  $(-H_0 + i\kappa/2)\mathbf{a} = \epsilon\mathbf{e}_1$ , where

$$H_0 = \begin{pmatrix} 0 & J & 0 & \cdots & 0 \\ J & 0 & J & \cdots & 0 \\ 0 & J & 0 & \cdots & 0 \\ \vdots & \vdots & \vdots & \ddots & J \\ 0 & 0 & 0 & J & 0 \end{pmatrix}, \quad \mathbf{e}_1 = \begin{pmatrix} 1 \\ 0 \\ 0 \\ \vdots \\ 0 \end{pmatrix}. \quad (\text{B3})$$

Defining the Green function as  $G = (-H_0 + i\kappa/2)^{-1}$ , the steady-state amplitude of the  $n$ -th mode can be expressed as [80]

$$b_n = \epsilon G_{n0}. \quad (\text{B4})$$

Consequently, the energy stored in the  $n$ -th battery is determined by the corresponding Green-function matrix element  $G_{n0}$ .

We can expand the Green function in the eigenbasis of the Hamiltonian by introducing the completeness relation

$$G = \sum_k \frac{1}{-E_k + i\kappa/2} |\psi_k\rangle\langle\psi_k|, \quad (\text{B5})$$

with  $E_k$  and  $\psi_k$  are the eigenvalues and eigenvectors of  $H$ ,  $\sum_k |\psi_k\rangle\langle\psi_k| = I$ . The corresponding matrix elements read

$$G_{ij} = \sum_k \frac{\psi_k(i)\psi_k(j)}{-E_k + i\kappa/2}, \quad (\text{B6})$$

where  $\psi_k(i) = \langle i|\psi_k\rangle$  and  $\psi_k(j) = \langle\psi_k|j\rangle$ .

Finally, the steady-state amplitude of the  $n$ -th battery is given explicitly by

$$b_n = \epsilon \sum_k \frac{\psi_k(n)\psi_k(0)}{-E_k + i\kappa/2}. \quad (\text{B7})$$

For an open chain of length  $L = N + 1$ , the eigenmodes of the tight-binding Hamiltonian are given by

$$\psi_k(n) = \sqrt{\frac{2}{L+1}} \sin\left(\frac{\pi k(n+1)}{L+1}\right), \quad (\text{B8})$$

with corresponding eigenvalues

$$E_k = 2J \cos\left(\frac{\pi k}{L+1}\right), \quad (\text{B9})$$

where  $k = 1, \dots, L$ . The eigenvector components at the first and last sites read

$$\psi_k(0) = \sqrt{\frac{2}{L+1}} \sin\left(\frac{\pi k}{L+1}\right), \quad (\text{B10})$$

$$\psi_k(N) = \sqrt{\frac{2}{L+1}} \sin\left(\frac{\pi kL}{L+1}\right). \quad (\text{B11})$$

Thus, using the Green-function expansion, the steady-state amplitude of the last battery is

$$b_N = \frac{2\epsilon}{L+1} \sum_k \frac{\sin\left(\frac{\pi k}{L+1}\right) \sin\left(\frac{\pi kL}{L+1}\right)}{-E_k + i\kappa/2}. \quad (\text{B12})$$

Applying the trigonometric identity

$$\sin\left(\frac{\pi kL}{L+1}\right) = (-1)^{k+1} \sin\left(\frac{\pi k}{L+1}\right), \quad (\text{B13})$$

we obtain

$$b_N = \frac{2\epsilon}{L+1} \sum_k \frac{(-1)^{k+1} \sin^2\left(\frac{\pi k}{L+1}\right)}{-E_k + i\kappa/2}. \quad (\text{B14})$$

The factor  $(-1)^{k+1}$  introduces alternating signs in the contributions from different eigenmodes.

For chains with an even number of batteries, one eigenmode appears close to zero energy, i.e.,  $E_k = 0$ , which strongly enhances the corresponding Green function term

$$\frac{1}{-E_k + i\kappa/2}. \quad (\text{B15})$$

This mode exhibits a large amplitude at the terminal sites, resulting in constructive energy transfer along the chain.

In contrast, for an odd number of batteries, the spectrum

is symmetric around zero energy, and no eigenmode exists exactly at  $E = 0$ . The contributions from different modes partially cancel due to the alternating sign  $(-1)^{k+1}$ , leading to destructive interference in the Green-function summation. Consequently, the steady-state amplitude at the last battery is smaller than in the even number case, i.e.,

$$|b_N|_{\text{even}} > |b_N|_{\text{odd}}, \quad (\text{B16})$$

which directly implies a larger stored energy.

- 
- [1] R. Alicki and M. Fannes, Entanglement boost for extractable work from ensembles of quantum batteries, *Phys. Rev. E* **87**, 042123 (2013).
- [2] F. C. Binder, S. Vinjanampathy, K. Modi, and J. Goold, Quantacell: powerful charging of quantum batteries, *New J. Phys.* **17**, 075015 (2015).
- [3] F. Campaioli, S. Gherardini, J. Q. Quach, M. Polini, and G. M. Andolina, Colloquium: Quantum batteries, *Rev. Mod. Phys.* **96**, 031001 (2024).
- [4] D. Ferraro, F. Cavaliere, M. G. Genoni, G. Benenti, and M. Sassetti, Opportunities and challenges of quantum batteries, *Nat. Rev. Phys.* **8**, 115 (2026).
- [5] H.-L. Shi, S. Ding, Q.-K. Wan, X.-H. Wang, and W.-L. Yang, Entanglement, coherence, and extractable work in quantum batteries, *Phys. Rev. Lett.* **129**, 130602 (2022).
- [6] J. Monsel, M. Fellous-Asiani, B. Huard, and A. Auffèves, The energetic cost of work extraction, *Phys. Rev. Lett.* **124**, 130601 (2020).
- [7] G. M. Andolina, D. Farina, A. Mari, V. Pellegrini, V. Giovannetti, and M. Polini, Charger-mediated energy transfer in exactly solvable models for quantum batteries, *Phys. Rev. B* **98**, 205423 (2018).
- [8] G. Francica, F. C. Binder, G. Guarnieri, M. T. Mitchison, J. Goold, and F. Plastina, Quantum coherence and ergotropy, *Phys. Rev. Lett.* **125**, 180603 (2020).
- [9] K. Hymas, J. B. Muir, D. Tibben, J. van Embden, T. Hirai, C. J. Dunn, D. E. Gómez, J. A. Hutchison, T. A. Smith, and J. Q. Quach, Superextensive electrical power from a quantum battery, *Light Sci. Appl.* **15**, 168 (2026).
- [10] M.-L. Song, Z. Cao, X.-K. Song, L. Ye, and D. Wang, Quantum steering as a probe of energy transfer in quantum batteries, *Phys. Rev. A* **113**, 022209 (2026).
- [11] A. E. Allahverdyan, R. Balian, and T. M. Nieuwenhuizen, Maximal work extraction from finite quantum systems, *Europhys. Lett.* **67**, 565 (2004).
- [12] G. M. Andolina, M. Keck, A. Mari, M. Campisi, V. Giovannetti, and M. Polini, Extractable work, the role of correlations, and asymptotic freedom in quantum batteries, *Phys. Rev. Lett.* **122**, 047702 (2019).
- [13] X. Yang, Y.-H. Yang, M. Alimuddin, R. Salvia, S.-M. Fei, L.-M. Zhao, S. Nimmrichter, and M.-X. Luo, Battery capacity of energy-storing quantum systems, *Phys. Rev. Lett.* **131**, 030402 (2023).
- [14] M. T. Mitchison, J. Goold, and J. Prior, Charging a quantum battery with linear feedback control, *Quantum* **5**, 500 (2021).
- [15] J.-s. Yan and J. Jing, Charging by quantum measurement, *Phys. Rev. Appl.* **19**, 064069 (2023).
- [16] J. Du, Y. Guo, and B. Li, Nonequilibrium quantum battery based on quantum measurements, *Phys. Rev. Res.* **7**, 013151 (2025).
- [17] A. C. Santos, B. i. e. i. f. m. c. Çakmak, S. Campbell, and N. T. Zinner, Stable adiabatic quantum batteries, *Phys. Rev. E* **100**, 032107 (2019).
- [18] F.-Q. Dou, Y.-J. Wang, and J.-A. Sun, Highly efficient charging and discharging of three-level quantum batteries through shortcuts to adiabaticity, *Front. Phys.* **17**, 31503 (2021).
- [19] C.-K. Hu, J. Qiu, P. J. P. Souza, J. Yuan, Y. Zhou, L. Zhang, J. Chu, X. Pan, L. Hu, J. Li, Y. Xu, Y. Zhong, S. Liu, F. Yan, D. Tan, R. Bachelard, C. J. Villas-Boas, A. C. Santos, and D. Yu, Optimal charging of a superconducting quantum battery, *Quantum Sci. Technol.* **7**, 045018 (2022).
- [20] J. Q. Quach, K. E. McGhee, L. Ganzer, D. M. Rouse, B. W. Lovett, E. M. Gauger, J. Keeling, G. Cerullo, D. G. Lidzey, and T. Virgili, Superabsorption in an organic microcavity: Toward a quantum battery, *Sci. Adv.* **8**, eabk3160 (2022).
- [21] G. Zhu, Y. Chen, Y. Hasegawa, and P. Xue, Charging quantum batteries via indefinite causal order: Theory and experiment, *Phys. Rev. Lett.* **131**, 240401 (2023).
- [22] D. Qu, X. Zhan, H. Lin, and P. Xue, Experimental optimization of charging quantum batteries through a catalyst system, *Phys. Rev. B* **108**, L180301 (2023).
- [23] Y. Ge, X. Yu, W. Xin, Z. Wang, Y. Zhang, W. Zheng, S. Li, D. Lan, and Y. Yu, Efficient charging and discharging of a superconducting quantum battery through frequency-modulated driving, *Appl. Phys. Lett.* **123**, 154002 (2023).
- [24] T. F. F. Santos, Y. V. de Almeida, and M. F. Santos, Vacuum-enhanced charging of a quantum battery, *Phys. Rev. A* **107**, 032203 (2023).
- [25] M.-L. Hu, T. Gao, and H. Fan, Efficient wireless charging of a quantum battery, *Phys. Rev. A* **111**, 042216 (2025).
- [26] F.-Q. Dou, H. Zhou, and J.-A. Sun, Cavity heisenberg-spin-chain quantum battery, *Phys. Rev. A* **106**, 032212 (2022).
- [27] R. R. Rodríguez, B. Ahmadi, G. Suárez, P. Mazurek, S. Barzanjeh, and P. Horodecki, Optimal quantum control of charging quantum batteries, *New J. Phys.* **26**, 043004 (2024).
- [28] C. A. Downing and M. S. Ukharty, Hyperbolic enhancement of a quantum battery, *Phys. Rev. A* **109**, 052206 (2024).
- [29] F. Campaioli, F. A. Pollock, F. C. Binder, L. Céleri, J. Goold, S. Vinjanampathy, and K. Modi, Enhancing the charging power of quantum batteries, *Phys. Rev. Lett.* **118**, 150601 (2017).
- [30] J.-Y. Gyhm, D. Šafránek, and D. Rosa, Quantum charging advantage cannot be extensive without global operations, *Phys. Rev. Lett.* **128**, 140501 (2022).
- [31] A. Rojo-Francàs, F. Isaule, A. C. Santos, B. Juliá-Díaz, and

- N. T. Zinner, Stable collective charging of ultracold-atom quantum batteries, *Phys. Rev. A* **110**, 032205 (2024).
- [32] G. M. Andolina, M. Keck, A. Mari, V. Giovannetti, and M. Polini, Quantum versus classical many-body batteries, *Phys. Rev. B* **99**, 205437 (2019).
- [33] T. P. Le, J. Levinsen, K. Modi, M. M. Parish, and F. A. Pollock, Spin-chain model of a many-body quantum battery, *Phys. Rev. A* **97**, 022106 (2018).
- [34] D. Ferraro, M. Campisi, G. M. Andolina, V. Pellegrini, and M. Polini, High-power collective charging of a solid-state quantum battery, *Phys. Rev. Lett.* **120**, 117702 (2018).
- [35] Y.-Y. Zhang, T.-R. Yang, L. Fu, and X. Wang, Powerful harmonic charging in a quantum battery, *Phys. Rev. E* **99**, 052106 (2019).
- [36] F.-Q. Dou, Y.-Q. Lu, Y.-J. Wang, and J.-A. Sun, Extended dicke quantum battery with interatomic interactions and driving field, *Phys. Rev. B* **105**, 115405 (2022).
- [37] S. S. Seidov and S. I. Mukhin, Quantum dicke battery supercharging in the bound-luminosity state, *Phys. Rev. A* **109**, 022210 (2024).
- [38] D. Rossini, G. M. Andolina, D. Rosa, M. Carrega, and M. Polini, Quantum advantage in the charging process of sachdev-ye-kitaev batteries, *Phys. Rev. Lett.* **125**, 236402 (2020).
- [39] P.-R. Lai, J.-D. Lin, Y.-T. Huang, H.-C. Jan, and Y.-N. Chen, Quick charging of a quantum battery with superposed trajectories, *Phys. Rev. Res.* **6**, 023136 (2024).
- [40] A. Crescente, M. Carrega, M. Sassetti, and D. Ferraro, Ultrafast charging in a two-photon dicke quantum battery, *Phys. Rev. B* **102**, 245407 (2020).
- [41] D.-L. Yang, F.-M. Yang, and F.-Q. Dou, Three-level dicke quantum battery, *Phys. Rev. B* **109**, 235432 (2024).
- [42] F. Pirmoradian and K. Mølmer, Aging of a quantum battery, *Phys. Rev. A* **100**, 043833 (2019).
- [43] J. Q. Quach and W. J. Munro, Using dark states to charge and stabilize open quantum batteries, *Phys. Rev. Appl.* **14**, 024092 (2020).
- [44] S.-Y. Bai and J.-H. An, Floquet engineering to reactivate a dissipative quantum battery, *Phys. Rev. A* **102**, 060201 (2020).
- [45] W.-L. Song, J.-L. Wang, B. Zhou, W.-L. Yang, and J.-H. An, Self-discharging mitigated quantum battery, *Phys. Rev. Lett.* **135**, 020405 (2025).
- [46] F. Barra, Dissipative charging of a quantum battery, *Phys. Rev. Lett.* **122**, 210601 (2019).
- [47] W.-L. Song, H.-B. Liu, B. Zhou, W.-L. Yang, and J.-H. An, Remote charging and degradation suppression for the quantum battery, *Phys. Rev. Lett.* **132**, 090401 (2024).
- [48] X. Huang, C. Lu, C. Liang, H. Tao, and Y.-C. Liu, Loss-induced nonreciprocity, *Light Sci. Appl.* **10**, 30 (2021).
- [49] B. Li, Y. Zuo, L.-M. Kuang, H. Jing, and C. Lee, Loss-induced quantum nonreciprocity, *npj Quantum Inf.* **10**, 75 (2024).
- [50] K. Xu, H.-J. Zhu, G.-F. Zhang, and W.-M. Liu, Enhancing the performance of an open quantum battery via environment engineering, *Phys. Rev. E* **104**, 064143 (2021).
- [51] K. V. Hovhannisyán, F. Barra, and A. Imparato, Charging assisted by thermalization, *Phys. Rev. Res.* **2**, 033413 (2020).
- [52] F. H. Kamin, F. T. Tabesh, S. Salimi, F. Kheirandish, and A. C. Santos, Non-markovian effects on charging and self-discharging process of quantum batteries, *New J. Phys.* **22**, 083007 (2020).
- [53] F. T. Tabesh, F. H. Kamin, and S. Salimi, Environment-mediated charging process of quantum batteries, *Phys. Rev. A* **102**, 052223 (2020).
- [54] F. H. Kamin, S. Salimi, and M. B. Arjmandi, Steady-state charging of quantum batteries via dissipative ancillas, *Phys. Rev. A* **109**, 022226 (2024).
- [55] J. Carrasco, J. R. Maze, C. Hermann-Avigliano, and F. Barra, Collective enhancement in dissipative quantum batteries, *Phys. Rev. E* **105**, 064119 (2022).
- [56] S. Ghosh, T. Chanda, S. Mal, and A. Sen(De), Fast charging of a quantum battery assisted by noise, *Phys. Rev. A* **104**, 032207 (2021).
- [57] F. Zhao, F.-Q. Dou, and Q. Zhao, Quantum battery of interacting spins with environmental noise, *Phys. Rev. A* **103**, 033715 (2021).
- [58] A. Metelmann and A. A. Clerk, Nonreciprocal photon transmission and amplification via reservoir engineering, *Phys. Rev. X* **5**, 021025 (2015).
- [59] Y.-X. Wang, C. Wang, and A. A. Clerk, Quantum nonreciprocal interactions via dissipative gauge symmetry, *PRX Quantum* **4**, 010306 (2023).
- [60] Y.-Y. Wang, Y.-X. Wang, S. van Geldern, T. Connolly, A. A. Clerk, and C. Wang, Dispersive nonreciprocity between a qubit and a cavity, *Sci. Adv.* **10**, eadj8796 (2024).
- [61] S. E. Begg and R. Hanai, Quantum criticality in open quantum spin chains with nonreciprocity, *Phys. Rev. Lett.* **132**, 120401 (2024).
- [62] X. Lu, W. Cao, W. Yi, H. Shen, and Y. Xiao, Nonreciprocity and quantum correlations of light transport in hot atoms via reservoir engineering, *Phys. Rev. Lett.* **126**, 223603 (2021).
- [63] B. Ahmadi, P. Mazurek, P. Horodecki, and S. Barzanjeh, Nonreciprocal quantum batteries, *Phys. Rev. Lett.* **132**, 210402 (2024).
- [64] B. Ahmadi, P. Mazurek, S. Barzanjeh, and P. Horodecki, Super-optimal charging of quantum batteries via reservoir engineering: Arbitrary energy transfer unlocked, *Phys. Rev. Appl.* **23**, 024010 (2025).
- [65] H.-W. Zhao, Y. Xie, X. Huang, and G.-F. Zhang, Enhanced charging in multibattery systems by nonreciprocity, *Phys. Rev. A* **112**, 022214 (2025).
- [66] Q.-Y. Lin, G.-Z. Ye, C. Li, W.-J. Su, and H.-Z. Wu, Enhanced charging power in nonreciprocal quantum battery by reservoir engineering, *Phys. Scr.* **101**, 025104 (2026).
- [67] E. I. R. Chiacchio, A. Nunnenkamp, and M. Brunelli, Nonreciprocal dicke model, *Phys. Rev. Lett.* **131**, 113602 (2023).
- [68] Y. Guo, L. Cao, and J. Zhao, Nonreciprocal open quantum battery network in a photonic waveguide array, *Phys. Rev. A* **111**, 063520 (2025).
- [69] C. Luan, C. Ma, C. Wang, L. Chang, L. Xiao, Z. Yu, and H. Li, Influence of the connection topology on the performance of lithium-ion battery pack under cell-to-cell parameters variations, *J. Energy Storage* **41**, 102896 (2021).
- [70] M. Ye, X. Song, R. Xiong, and F. Sun, A novel dynamic performance analysis and evaluation model of series-parallel connected battery pack for electric vehicles, *IEEE Access* **7**, 14256 (2019).
- [71] Y.-Q. Liu, Y.-J. Yang, Z. Liu, B.-Q. Guo, T.-T. Ma, Z.-L. Zhu, W.-M. Liu, X.-D. Zhao, and C.-S. Yu, Dissipative quantum battery in the ultrastrong coupling regime between two oscillators, arXiv preprint arXiv:2602.15235 (2026).
- [72] F. Centrone, L. Mancino, and M. Paternostro, Charging batteries with quantum squeezing, *Phys. Rev. A* **108**, 052213 (2023).
- [73] J. Yang, S. Fang, C. Zhao, C. Shan, and B. Xiong, Quantum battery via reservoir engineering, *Phys. Rev. Appl.* **25**, 034013 (2026).
- [74] Y. Li, R.-F. Liu, J.-B. You, W.-L. Yang, and H. Guan, Enhancing the performance of quantum battery by squeezing reservoir engineering, *Chinese Phys. B* **35**, 010303 (2026).

- [75] A. E. Allahverdyan, R. Balian, and T. M. Nieuwenhuizen, Maximal work extraction from finite quantum systems, *Europhys. Lett.* **67**, 565 (2004).
- [76] Z. Niu, Y. Wu, Y. Wang, X. Rong, and J. Du, Experimental investigation of coherent ergotropy in a single spin system, *Phys. Rev. Lett.* **133**, 180401 (2024).
- [77] R. R. Rodríguez, B. Ahmadi, P. Mazurek, S. Barzanjeh, R. Al-icki, and P. Horodecki, Catalysis in charging quantum batteries, *Phys. Rev. A* **107**, 042419 (2023).
- [78] T. K. Konar, L. G. C. Lakkaraju, and A. Sen (De), Quantum battery with non-hermitian charging, *Phys. Rev. A* **109**, 042207 (2024).
- [79] B.-B. Liu, R. Chen, J.-L. Wu, G. Chen, and S.-L. Su, Data for the paper “Connection topology-dependent energy transport and ergotropy in quantum battery networks with reciprocal and nonreciprocal couplings”, [10.5281/zenodo.19182043](https://zenodo.org/record/19182043) (2026).
- [80] E. N. Economou, *Green's functions in quantum physics* (Springer, 2006).